

Influence of 2p-2h configurations on β -decay rates

A. P. Severyukhin,¹ V. V. Voronov,¹ I. N. Borzov,¹ N. N. Arsenyev,¹ and Nguyen Van Giai²

¹*Bogoliubov Laboratory of Theoretical Physics, Joint Institute for Nuclear Research, 141980 Dubna, Moscow region, Russia*

²*Institut de Physique Nucléaire, CNRS-IN2P3 and Univ. Paris-Sud, 91405 Orsay, France*

(Dated: June 26, 2014)

The effects of the phonon-phonon coupling on the β -decay rates of neutron-rich nuclei are studied in a microscopic model based on Skyrme-type interactions. The approach uses a finite-rank separable approximation (FRSA) of the Skyrme-type particle-hole (p-h) residual interaction. Very large two-quasiparticle spaces can thus be treated. A redistribution of the Gamow-Teller (G-T) strength is found due to the tensor correlations and the $2p - 2h$ fragmentation of G-T states. As a result, the β^- -decay half-lives are decreased significantly. Using the Skyrme interaction SGII together with a volume-type pairing interaction we illustrate this reduction effect by comparing with available experimental data for the Ni isotopes and neutron-rich $N = 50$ isotones. We give predictions for ^{76}Fe and ^{80}Ni in comparison with the case of the doubly-magic nucleus ^{78}Ni which is an important waiting point in the r-process.

PACS numbers: 21.60.Jz, 23.40.-s, 21.60.Ev, 21.10.Re

I. INTRODUCTION

Many fundamental nuclear physics issues depend on our quantitative understanding of the β -decay phenomena in nuclei. Due to phase-space amplification effects, the β -decay rates are sensitive to both nuclear binding energies and β -strength functions. Within an appropriate β -decay model, the correct amount of the integral β -strength should be placed within the properly calculated Q_{β^-} window provided that the spectral distribution is also close to the "true" β -strength function. It is desirable to have theoretical models which can describe the data wherever they can be measured, and predict the properties related to spin-isospin modes in the nuclei too short-lived to allow for experimental studies. One of the successful tools for studying charge-exchange nuclear modes is the quasiparticle random phase approximation (QRPA) with the self-consistent mean-field derived from a Skyrme-type energy-density functional (EDF), see e.g., [1–8]. These QRPA calculations enable one to describe the properties of the ground state and excited charge-exchange states using the same EDF.

Experimental studies using the multipole decomposition analysis of the (n,p) and (p,n) reactions [9, 10] found substantial Gamow-Teller (G-T) strength above the G-T resonance peak and have clarified a longstanding problem of the missing experimental G-T strength, hence resolving the discrepancies between the theoretical RPA predictions and the experimental measurements. It has been found necessary to take into account the coupling with more complex configurations in order to shift some strength to higher energies and to comply with the experimental results [11–13]. Using the Skyrme EDF and the RPA, such attempts in the past [14, 15] have allowed one to understand the damping of charge-exchange resonances and their particle decay. Recently, the damping of the G-T mode has been investigated using the Skyrme-RPA plus particle-vibration coupling [16]. The main difficulty is that the complexity of the calculations increases

rapidly with the size of the configuration space and one has to work within limited spaces.

Making use of the finite rank separable approximation (FRSA) [17–19] for the residual interaction one can perform Skyrme-QRPA calculations in very large two-quasiparticle spaces. Following the basic ideas of the quasiparticle-phonon model (QPM) [20], the approach has been generalized for the coupling between one- and two-phonon components of the wave functions [21]. The so-called FRSA was thus used to study the electric low-lying states and giant resonances within and beyond the QRPA [19, 21, 22].

Recently, the FRSA approach was extended to charge-exchange nuclear excitations [23] and also for accommodating the tensor correlations which mimic the Skyrme-type tensor interactions [24]. In the present work we generalize the approach to the coupling between one- and two-phonon components in the wave functions. As an application of the method we study the β -decay half-lives of neutron-rich $N = 50$ isotones and Ni isotopes and we compare to the most neutron-rich ($(N - Z)/A = 0.28$) doubly-magic nucleus ^{78}Ni which is also an important waiting point in the r-process [25]. In the case of ^{78}Ni preliminary results of our calculation without the tensor interaction are already reported in Ref. [26].

This paper is organized as follows. In Sec. II, we sketch the method for including the effects of the phonon-phonon coupling. In Sec. III, we discuss the details of QRPA calculations for the 1^+ states of the daughter nuclei and the 2^+ states of the parent nuclei. In Sec. IV, we analyze the results of the calculations of β -decay rates. Conclusions are finally drawn in Sec. V.

II. THE FRSA MODEL

The FRSA model for charge-exchange excitations was already introduced in Refs. [23, 24]. In the present study, this method is extended by including the coupling

between one- and two-phonon terms in the wave functions of G-T states. The starting point is the Hartree-Fock(HF)-BCS calculation [27] of the parent ground state within a spherical symmetry assumption. In the particle-hole (p-h) channel we use the Skyrme interaction with the triplet-even and triplet-odd tensor components introduced in Refs. [28, 29]. The continuous part of the single-particle spectrum is discretized by diagonalizing the HF hamiltonian on a harmonic oscillator basis. The inclusion of the tensor interaction results in the following modification of the spin-orbit potential in coordinate space [30, 31]:

$$U_{S.O.}^{(q)} = \frac{W_0}{2r} \left(2 \frac{d\rho_q}{dr} + \frac{d\rho_{q'}}{dr} \right) + \left(\alpha \frac{J_q}{r} + \beta \frac{J_{q'}}{r} \right), \quad (1)$$

where ρ_q and J_q ($q = n, p$) are the densities and the spin-orbit densities, respectively. The coefficients α and β can be separated into contributions from the central force (α_c, β_c) and the tensor force (α_T, β_T) [30, 31]. The pairing correlations are generated by the density-dependent zero-range force

$$V_{pair}(\mathbf{r}_1, \mathbf{r}_2) = V_0 \left(1 - \eta \left(\frac{\rho(r_1)}{\rho_0} \right)^\gamma \right) \delta(\mathbf{r}_1 - \mathbf{r}_2), \quad (2)$$

where ρ_0 is the nuclear saturation density. The values of V_0 , η and γ are fixed to reproduce the odd-even mass difference of the studied nuclei [19].

To build the QRPA equations on the basis of HF-BCS quasiparticle states with the residual interactions consistently derived from the Skyrme EDF in the p-h channel and from the zero-range pairing force in the particle-particle (p-p) channel is a standard procedure [32]. The dimensions of the QRPA matrix grow very rapidly with the size of the nuclear system unless severe and damaging cut-offs are made to the 2-quasiparticle configuration space. It is well known that, if the QRPA matrix elements take a separable form the QRPA energies can be obtained as the roots of a relatively simple secular equation [20, 33]. In the case of the Skyrme interaction this feature has been exploited by different authors [17, 34, 35].

The main step of the FRSA is to simplify the central p-h interaction V_{ph}^C by approximating it by its Landau-Migdal form. All Landau parameters with $l > 1$ are equal to zero in the case of Skyrme interactions. We keep only the $l = 0$ terms in V_{ph}^C and this approximation is reasonable [17, 19]. The two-body Coulomb residual interaction is dropped. Therefore we can write V_{ph}^C as

$$V_{res}^a(\mathbf{r}_1, \mathbf{r}_2) = N_0^{-1} [F_0^a(r_1) + G_0^a(r_1)\sigma_1 \cdot \sigma_2 + (F_0'^a(r_1) + G_0'^a(r_1)\sigma_1 \cdot \sigma_2)\tau_1 \cdot \tau_2] \delta(\mathbf{r}_1 - \mathbf{r}_2), \quad (3)$$

where a is the channel index $a = \{ph, pp\}$; σ_i and τ_i are the spin and isospin operators, $N_0 = 2k_F m^* / \pi^2 \hbar^2$ with the Fermi momentum k_F and m^* is the nucleon effective mass. The coefficients G_0^{pp} and $G_0'^{pp}$ are zero, while the

expressions for F_0^{ph} , $F_0'^{ph}$, G_0^{ph} , $G_0'^{ph}$ and F_0^{pp} , $F_0'^{pp}$ can be found in Ref. [36] and in Ref. [19], respectively. For the case of electric excitations one can neglect the spin-spin terms since they play a minor role. Though it is well known that the p-p interaction in the spin-isospin channel ($T = 0$ pairing) suppresses the β^- -decay half-lives, in the present study we assume $G_0'^{pp} = 0$ in order to separate the sole impact of the tensor force. As proposed in Refs. [24, 37], we simplify the tensor p-h interaction by replacing it by the two-term separable interaction, where the strength parameters are adjusted to reproduce the centroid energies of the G-T and spin-quadrupole strength distributions calculated with the original tensor p-h interaction.

The p-h matrix elements and the antisymmetrized p-p matrix elements can be written in a separable form in the space of the angular coordinates [17, 19]. After integrating over the angular variables the one-dimensional radial integrals are numerically calculated by choosing a large enough cutoff radius R and using an N -point integration Gauss formula with abscissas r_k and weights w_k [17]. Thus, one is led to deal with a problem where the matrix elements of the residual interaction are sums of products and the number \tilde{N} of terms in the sums depends only on N . In particular, $\tilde{N} = 4N + 4$ and $\tilde{N} = 6N$ are obtained for the cases of G-T and electric excitations, respectively. One can call it a separable approximation of finite rank \tilde{N} since finding the roots of the secular equation amounts to find the zeros of a $\tilde{N} \times \tilde{N}$ determinant, and the dimensions of the determinant are independent of the size of the configuration space, i.e., of the nucleus considered. The studies of Refs. [19, 23] enable us to conclude that $N=45$ is enough for the electric and charge-exchange excitations considered here in nuclei with $A \leq 208$.

In the next step, we construct the wave functions from a linear combination of one-phonon and two-phonon configurations

$$\Psi_\nu(JM) = \left(\sum_i R_i(J\nu) Q_{JM_i}^+ + \sum_{\lambda_1 i_1 \lambda_2 i_2} P_{\lambda_2 i_2}^{\lambda_1 i_1}(J\nu) \left[Q_{\lambda_1 \mu_1 i_1}^+ \bar{Q}_{\lambda_2 \mu_2 i_2}^+ \right]_{JM} \right) |0\rangle, \quad (4)$$

where $Q_{\lambda \mu i}^+ |0\rangle$ ($\bar{Q}_{\lambda \mu i}^+ |0\rangle$) is the G-T (electric) excitation having energy $\omega_{\lambda i}$ ($\bar{\omega}_{\lambda i}$). The normalization condition for the wave functions (4) is

$$\sum_i R_i^2(J\nu) + \sum_{\lambda_1 i_1 \lambda_2 i_2} (P_{\lambda_2 i_2}^{\lambda_1 i_1}(J\nu))^2 = 1. \quad (5)$$

The amplitudes $R_i(J\nu)$ and $P_{\lambda_2 i_2}^{\lambda_1 i_1}(J\nu)$ are determined from the variational principle which leads to a set of linear equations

$$(\omega_{\lambda i} - \Omega_\nu) R_i(J\nu) + \sum_{\lambda_1 i_1 \lambda_2 i_2} U_{\lambda_2 i_2}^{\lambda_1 i_1}(J\nu) P_{\lambda_2 i_2}^{\lambda_1 i_1}(J\nu) = 0, \quad (6)$$

$$\begin{aligned}
& (\omega_{\lambda_1 i_1} + \bar{\omega}_{\lambda_2 i_2} - \Omega_\nu) P_{\lambda_2 i_2}^{\lambda_1 i_1}(J\nu) \\
& + \sum_i U_{\lambda_2 i_2}^{\lambda_1 i_1}(Ji) R_i(J\nu) = 0. \quad (7)
\end{aligned}$$

The rank of the set of linear equations (6) and (7) is equal to the number of one- and two-phonon configurations included in the wave function (4). For its solution it is required to compute the Hamiltonian matrix elements coupling one- and two-phonon configurations

$$U_{\lambda_2 i_2}^{\lambda_1 i_1}(Ji) = \langle 0 | Q_{Ji} H [Q_{\lambda_1 i_1}^+ \bar{Q}_{\lambda_2 i_2}^+]_J | 0 \rangle. \quad (8)$$

Eqs. (6) and (7) have the same form as the QPM equations [12, 20], where the single-particle spectrum and the residual interaction are derived from the same Skyrme EDF.

In the allowed G-T approximation, the β^- -decay rate is expressed by summing the probabilities of the energetically allowed G-T transitions (in units of $G_A^2/4\pi$) weighted with the integrated Fermi function

$$\begin{aligned}
T_{1/2}^{-1} &= \sum_m \lambda_{if}^m = D^{-1} \left(\frac{G_A}{G_V} \right)^2 \times \\
&\sum_m f_0(Z, A, E_i - E_{1_m^+}) B(G-T)_m, \quad (9)
\end{aligned}$$

$$E_i - E_{1_m^+} \approx \Delta M_{n-H} + \mu_n - \mu_p - E_m, \quad (10)$$

where λ_{if}^m is the partial β^- -decay rate, $G_A/G_V=1.25$ [38] is the ratio of the weak axial-vector and vector coupling constants and $D=6147$ s (see Ref. [38]). $\Delta M_{n-H} = 0.782$ MeV is the mass difference between the neutron and the hydrogen atom, μ_n and μ_p are the neutron and proton chemical potentials, respectively, E_i is the ground state energy of the parent nucleus, and $E_{1_m^+}$ denotes a state of the daughter nucleus (Z, A). E_m and $B(G-T)_m$ are the solutions either of the QRPA equations, or of Eqs. (6)-(7) taking into account the two-phonon configurations.

Thus, to calculate the half-lives by Eqs.(9) and (10) an approximation worked out in Ref. [2] is used. It allows one to avoid an implicit calculation of the nuclear masses and Q_β -values. However, one should realize that the related uncertainty in constraining the parent nucleus ground state calculated with the chosen Skyrme interaction is transferred to the values of the neutron and proton chemical potentials entering Eq. (10).

III. DETAILS OF CALCULATIONS

We apply the approach to study the influence of the coupling between one- and two-phonon terms in the wave functions, as well as the tensor force effects on the strength distributions of G-T states in the neutron-rich Ni isotopes and $N = 50$ isotones. To obtain the interaction in the p-h channel, we use the Skyrme interaction SGII [36] and the zero-range tensor interaction of

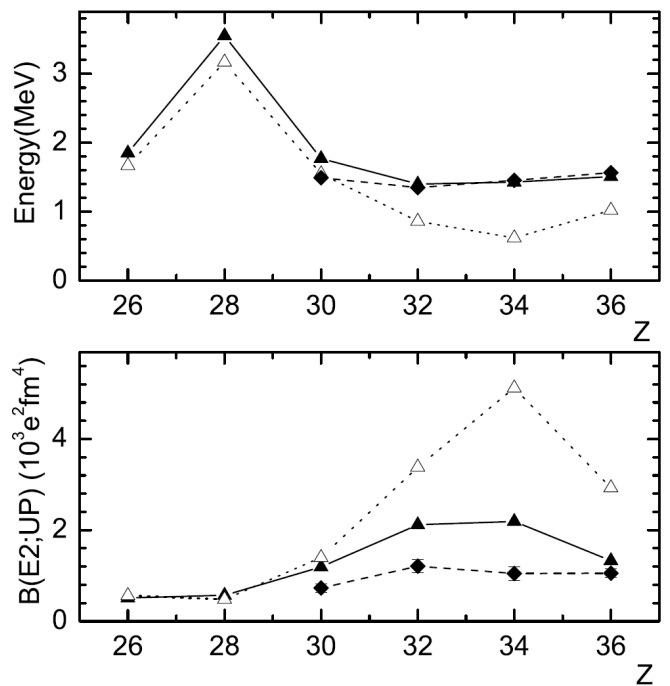


FIG. 1: Energies and $B(E2)$ values for up-transitions to the $[2_1^+]_{QRPA}$ states in the neutron-rich $N = 50$ isotones. Results of the calculations without the tensor interaction (open triangles) and with the tensor interaction (filled triangles) are shown. Experimental data (filled diamonds) are taken from Ref. [41].

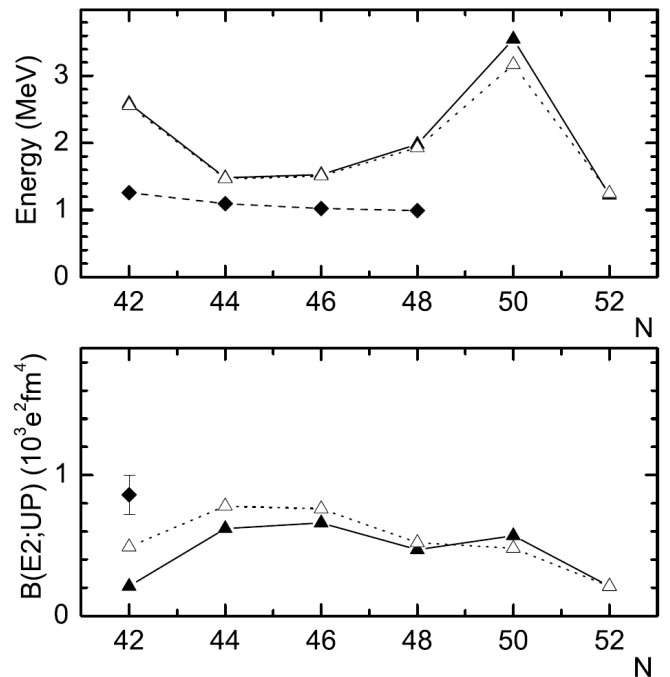


FIG. 2: Same as Fig. 1, but for the neutron-rich Ni isotopes

Ref. [37] with $\alpha_T=-180$ MeVfm⁵ and $\beta_T=120$ MeVfm⁵

for the parameters α and β of the one-body spin-orbit potential of Eq.(1).

Since the SGII parametrization gives reasonable values for the Landau parameters $F'_0 = 0.73$ and $G'_0 = 0.50$, one obtains a successful description of the spin-dependent properties, in particular for the experimental energies of the G-T resonances of ^{90}Zr [36]. In Ref. [24], the FRSA model has been used to calculate the G-T states of ^{90}Zr and ^{208}Pb , and the FRSA results reproduce the main features of the G-T strength distributions obtained with the exact treatment of Skyrme tensor interactions in the RPA.

For the interaction in the p-p channel, we use a zero-range volume force, i.e., $\eta = 0$ in Eq. (2) and $V_0 = -270 \text{ MeVfm}^3$ with a smooth cut-off at 10 MeV above the Fermi energies [19, 39]. This value of the pairing strength has been fitted to reproduce the experimental pairing energies of $^{70,72,74,76}\text{Ni}$ obtained from binding energies of neighbouring nuclei. This choice of the pairing interaction has also been used for a satisfactory description of the experimental data of $^{90,92}\text{Zr}$ and $^{92,94}\text{Mo}$ [22]. Because of the closed $Z = 28$ and $N = 50$ shells, the $T = 0$ pairing is not effective in these nuclei [40] and, therefore, it can be neglected.

We now use the FRSA of the residual interaction and carry out QRPA calculations in very large two-quasiparticle spaces. In particular, the cut-off in the discretized continuous part of the s.p. spectra is at 100 MeV. Because of the inclusion of the tensor correlation effects within the $1p - 1h$ and $2p - 2h$ configuration space, we do not need any quenching factor [11]. For the ansatz of the wave function (4), the Ikeda sum rule $S_- - S_+ = 3(N - Z)$ is fulfilled, see e.g., [12]. Our configurational space is sufficient to exhaust this sum rule for the G-T strength of the nuclei that we studied without and with the tensor force. As an illustrative example, in the case taking into account the tensor correlations for $^{82}_{32}\text{Ge}$ we obtain $S_- = 56.85$ and $S_+ = 2.84$ in the QRPA, the inclusion of the 2p-2h effects gives the same values. The results without the tensor interaction indicate $S_- = 54.46$ and $S_+ = 0.45$.

Let us now focus on the properties of the low-energy G-T state, since we are interested in the β -decay half-lives. Its experimentally known half-life puts an indirect constrain on the calculated G-T strength distributions within the Q_β -window. Let us examine the extension of the configuration space to one- and two-phonon terms. To construct the wave functions (4) of the low-lying 1^+ states we use only the $[1_i^+ \otimes \lambda_\nu^+]_{QRPA}$ terms and all electric phonons with $\lambda > 2$ vanish, i.e., G-T phonons from the charge-exchange modes are only used in the two-phonon terms, as in Ref. [14, 16]. All one- and two-phonon configurations with the transition energies $|E_{1_m^+} - E_i|$ up to 10 MeV are included. We have checked that the inclusion of the high-energy configurations leads to minor effects on the half-life values.

It is interesting to study the energies, reduced transition probabilities and the structure of the 2^+_1 QRPA

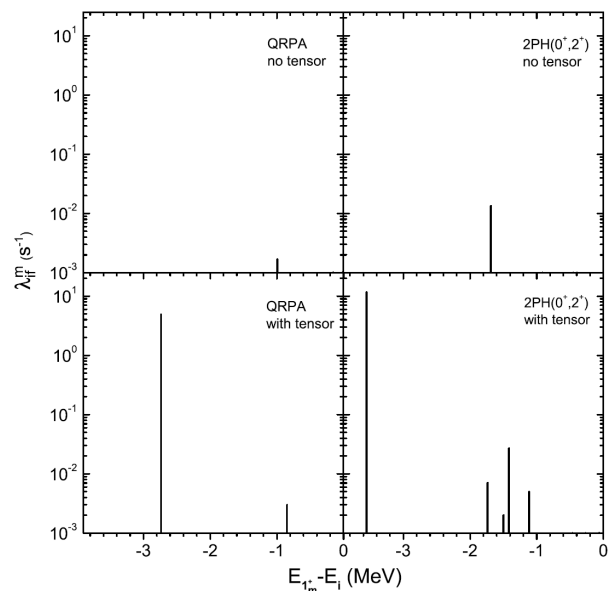


FIG. 3: The phonon-phonon coupling effect on the β -transition rates in ^{80}Zn . The left and right panels correspond to the calculations within the QRPA and taking into account the $2p - 2h$ configurations, respectively. Results of the calculations without (resp. with) the tensor interaction are shown in the upper (resp. lower) panels.

state. The calculated 2^+_1 energies and transition probabilities in the neutron-rich $N = 50$ isotones are compared with existing experimental data [41] in Fig.1. The FRSA model with the tensor interaction reproduces the experimental data [41] very well. We find that the tensor interaction induces a reduction of the 2^+_1 collectivity and it results in a decrease of the transition probability, see Fig.1. There is a remarkable increase of the 2^+_1 energy of ^{78}Ni in comparison with those in ^{76}Fe and ^{80}Zn . It corresponds to a standard evolution of the 2^+_1 energy near closed shells. As can be seen from Fig.2, the behavior of 2^+_1 energies of $^{76,78,80}\text{Ni}$ is similar to that of the $N = 50$ isotones. It is seen that the inclusion of the tensor interaction does not change energies and transition probabilities along this Ni isotopic chain except for ^{70}Ni . Including the tensor interaction changes contributions of the main configurations only slightly, but the general structure of the 2^+_1 state remains the same. The neutron amplitudes are dominant in all Ni isotopes and the contribution of the main neutron configuration $\{1g_{9/2}, 1g_{9/2}\}$ decreases from 89% for ^{70}Ni to 77% for ^{76}Ni when neutrons fill the subshell $1g_{9/2}$. Thus, a satisfactory description of 2^+_1 energies is found for $^{72,74,76}\text{Ni}$. Our calculated 2^+_1 energy of ^{70}Ni is about a factor of 2 too large compared to the data value [41]. This is likely due to the overestimation of the neutron contribution to the 2^+_1 wave function within the QRPA. One can expect some improvement if the coupling with the two-phonon components of the wave functions is taken into account [21, 22].

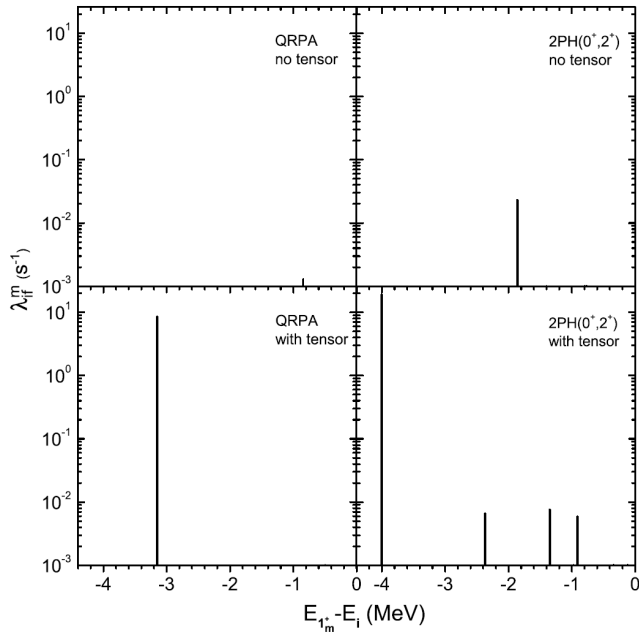


FIG. 4: Same as Fig. 3, but for ^{72}Ni .

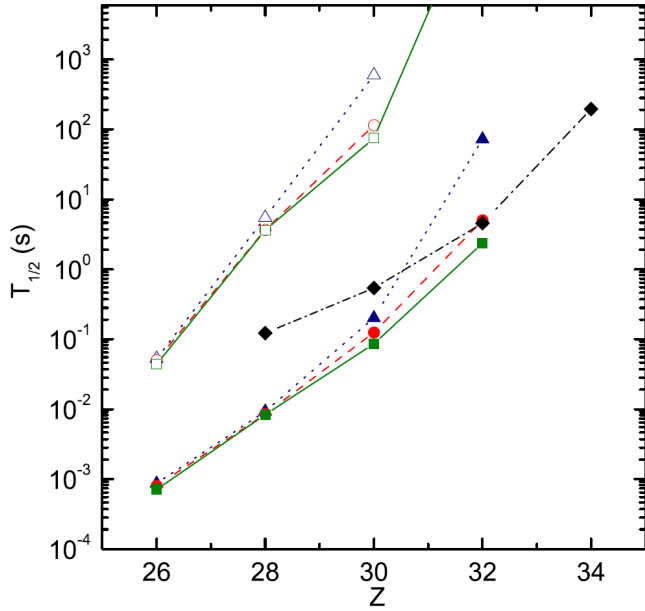


FIG. 5: The phonon-phonon coupling effect on β^- -decay half-lives of the neutron-rich $N = 50$ isotones. Results of the calculations without the tensor interaction (open triangles, circles, squares) and with the tensor interaction (filled triangles, circles, squares) are shown. The squares correspond to the half-lives calculated with inclusion of the phonon-phonon coupling, the triangles are the QRPA calculations. Results including the $[1_i^+ \otimes 2_{if}^+]_{QRPA}$ configurations are denoted by the circles. Experimental data (filled diamonds) are from Refs. [43, 44].

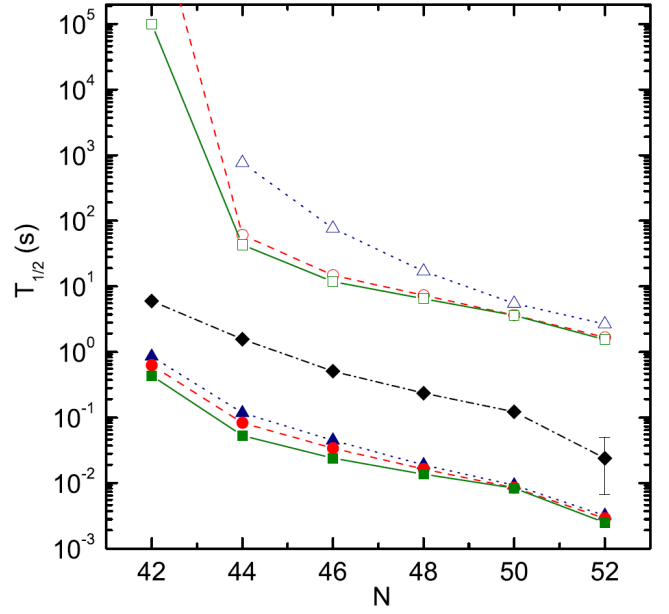


FIG. 6: Same as Fig. 5, but for the neutron-rich Ni isotopes. Experimental data are taken from Refs. [42–44].

IV. RESULTS FOR β^- -DECAY RATES

Using the same set of parameters we calculate the low-lying G-T strength distributions of the neutron-rich nuclei ^{76}Fe , $^{70,72,74,76,78,80}\text{Ni}$, ^{80}Zn , ^{82}Ge and ^{84}Se . First, the properties of the low-lying 1^+ states of the daughter nuclei are studied within the one-phonon approximation. As expected, the largest contribution ($>88\%$) in the calculated β^- -decay half-life comes from the $[1_1^+]_{QRPA}$ state. To illustrate it, the β -transition rates λ_{if}^m of ^{80}Zn and ^{72}Ni are shown in Fig. 3 and Fig. 4, respectively. The transition energies $E_{1_m^+} - E_i$ refer to the ground state of the parent nucleus.

QRPA results calculated without the tensor interaction indicate that the dominant configuration of the $[1_1^+]_{QRPA}$ states is $\{\pi 2p_{3/2}^3 \nu 2p_{1/2}^1\}$ whose contribution is about 91% in all the cases considered. In other words, the $[1_1^+]_{QRPA}$ state is not collective and, therefore, the β^- -decay is related to the unperturbed $\{\pi 2p_{3/2}^3 \nu 2p_{1/2}^1\}$ energy. At the same time the calculated $\log ft$ value increases from 3.7 for ^{72}Ni to 3.9 for ^{80}Ni . The β^- -decay half-lives of the neutron-rich $N = 50$ isotones and the Ni isotopes are shown in Fig. 5 and Fig. 6, respectively. The calculated values overestimate the experimental data [25, 42–44]. Moreover, for ^{70}Ni , ^{82}Ge and ^{84}Se , the $[1_1^+]_{QRPA}$ state of the daughter nucleus is above the parent ground state, i.e., this calculation predicts stable ^{70}Ni , ^{82}Ge and ^{84}Se . It is worth pointing out that the relativistic QRPA approach [40] gives a similar structure of the $[1_1^+]_{QRPA}$ state for these nuclei.

As a general trend, we observe a redistribution of the G-T strengths by the inclusion of the tensor interaction in the QRPA, in the same way as it was found in

Refs. [6, 7, 24]. The tensor correlations shift up about 10% of the G-T strength to the energy region above 30MeV. Also, the tensor interaction makes a downward shift of the strength in the G-T resonance region below the peak energy and the $[1_1^+]_{QRPA}$ state is moved downwards. This is illustrated in the cases of ^{80}Zn and ^{72}Ni (see left bottom panels of Figs. 3-4). For ^{80}Ni , the $[1_1^+]_{QRPA}$ energy shift reaches 2.7 MeV. In particular, because of this shift, we get unstable ^{70}Ni and ^{82}Ge . In addition, the tensor correlations lead to a collective structure for the $[1_1^+]_{QRPA}$ state with the dominance of the $\{\pi 2p_{3/2}^2 \nu 2p_{3/2}^2\}$ configuration. In the case of the $N = 50$ isotones the $\{\pi 2p_{3/2}^2 \nu 2p_{3/2}^2\}$ contribution increases from 46% in ^{78}Ni to 72% in ^{84}Se , whereas for Ni isotopes this contribution decreases from 57% in ^{70}Ni to 39% in ^{80}Ni . The $[1_1^+]_{QRPA}$ collectivity is reflected in the $\log ft$ value and there is a slight decrease of the $\log ft$ from 2.3 for ^{70}Ni to 2.0 for ^{80}Ni . As can be seen from Fig.5 and Fig.6, the half-lives calculated with the tensor force are about 60-2000 times shorter than those calculated without. This analysis within the one-phonon approximation can help to identify the tensor correlation effects, but it is only a rough estimate. It is worth to mention that the first discussion of the strong impact of the tensor correlations on the β^- -decay half-lives based on QRPA calculations with Skyrme forces has been done in Ref. [8].

Let us now discuss the extension of the space to one- and two-phonon configurations in the FRSA model when the tensor interaction is taken into account. In all ten nuclei, the dominant contribution in the wave function of the first 1^+ state comes from the $[1_1^+]_{QRPA}$ configuration, but the two-phonon contributions are appreciable. The main two-phonon components of the 1_1^+ wave function are the $[1_1^+ \otimes 2_1^+]_{QRPA}$ and $[1_1^+ \otimes 0_2^+]_{QRPA}$ configurations. When the tensor interaction is not included, the main configuration is only the $[1_1^+ \otimes 2_1^+]_{QRPA}$ configuration. As a result, the inclusion of the two-phonon terms results in an increase of the transition energies $|E_{1_1^+} - E_i|$ and the energy shift is large (1.1 MeV for ^{82}Ge and 0.8 MeV for ^{80}Zn) in comparison with 0.2 MeV in the case of the doubly-magic nucleus ^{78}Ni . The $\log ft$ value is practically unchanged. One can see from Figs.5-6 that the effects of the phonon-phonon coupling produce a sizable impact on the β -decay half-life which is reduced by a factor 30. Specifically, the $[1_1^+ \otimes 2_1^+]_{QRPA}$ configuration is the important ingredient for the half-life description since the $[2_1^+]_{QRPA}$ state is the lowest collective-electromagnetic excitation which leads to the minimal two-phonon energy and the maximal matrix elements coupling one- and two-phonon configurations of Eqs. (6) and (7). Figs. 5 and 6 also show the half-life reduction as an effect of the quadrupole-phonon coupling. For ^{84}Se , the experimental half-life is $T_{1/2} = 3.26 \pm 0.10$ min[43], but our model predicts that this nucleus is stable against β -decay and, in particular, $E_{1_1^+} - E_i = 0.0$ MeV. One can expect an improvement if the $T = 0$ pairing interaction is taken into account. We intend to extend our formalism

to include the $T = 0$ pairing effects.

It is interesting to discuss the change of the half-lives along the chains of the $N = 50$ isotones and the Ni isotopes. As pointed out in Refs. [42–44], there are different evolutions of the existing experimental half-lives, namely, the 37.3-time reduction of half-life values from ^{82}Ge to ^{78}Ni and the gradual reduction of half-lives with increasing neutron number for the Ni isotopes. One can see that our results reproduce this behaviour which is sensitive to the isotopic and isotonic dependences of the transition energies $|E_{1_1^+} - E_i|$. We find that the energy $|E_{1_1^+} - E_i|$ for ^{82}Ge (^{74}Ni) is 3.1 (1.2) times less than that in ^{78}Ni . It is worth to mention that the calculated half-life of ^{82}Ge is in reasonable agreement with the experimental data. As can be seen from Fig. 6, the main discrepancies between measured and calculated half-lives of Ni isotopes are due to too strong tensor correlations and one should seek for improvements in the tensor part of the effective interaction used. Finally, for neighbours of ^{78}Ni we give predictions as the bottom limit of the half-life (0.7 ms for ^{76}Fe and 2.5 ms for ^{80}Ni). It is seen that the phonon-phonon coupling plays a minor role. Our calculated half-life of ^{80}Ni is in qualitative agreement with the recently observed value of $23.9_{-17.2}^{+26.0}$ ms [44].

The SGII parametrization of the central force gives a reasonable description of properties of the G-T and charge-exchange spin-dipole resonances of ^{90}Zr [7, 36] and the low-energy spectrum of the quadrupole excitations for nuclei near ^{90}Zr [22]. For the half-life description, the quantitative agreement with the experimental data is not satisfactory for the neutron-rich nuclei. A possible reason might be the underestimated symmetry energy of 26.8 MeV in the case of the SGII set. A half-life study of the influence of the two-phonon terms with taking into account the tensor interaction for the different parametrizations of central Skyrme force is still underway.

Inclusion of the tensor interaction results in significant increase of the transition energies and partial rates of the main G-T transitions. Including the $2p - 2h$ configurations leads to further increase of its rate and to the appearance of the weak fragmented satellites at low transition energy (see, e.g., right bottom panels of Figs.3-4). Importantly, such a change of the G-T strength distribution takes place in the near-threshold region. Thus, an additional constraint on the β -strength distribution is also given by delayed neutron emission probability (P_n -value) [45]. Since the FRSA model enables one to evaluate the coupling of QRPA phonons to more complex configurations, such calculations that take into account the $2p - 2h$ fragmentation of the QRPA excitations are now in progress.

V. CONCLUSIONS

Starting from a Skyrme effective interaction the G-T strength in the Q_β - window has been studied within

the extended FRSA model including both the tensor interaction and $2p - 2h$ configurations effects. The suggested approach enables one to perform the calculations in very large configuration spaces. Using the parameter set SGII+tensor interaction, we have applied this model to the G-T states in the neutron-rich Ni isotopes and $N = 50$ isotones, for which experimental data of β^- -decay rates are available. The inclusion of the tensor interaction leads to a redistribution of the G-T strength. The low-energy G-T strength is fragmented and the 1_1^+ state is moved downwards. We observe that the coupling between one- and two-phonon terms with the 2^+ phonon states is strong in these nuclei, and the $2p - 2h$ fragmentation and damping of the QRPA excitations are thus important. In particular, the energy shift of the lowest 1^+ state due to the phonon-phonon coupling is large: 0.8 MeV in ^{80}Zn and 1.1 MeV in ^{82}Ge in comparison with 0.2 MeV in the case of ^{78}Ni . Taking into account these effects results in a dramatic reduction of β -decay half-lives. It is shown that the $2p - 2h$ impact on the half-lives comes inherently from the $[1_1^+ \otimes 2_1^+]_{QRPA}$ term of the wave function of the 1_1^+ state. At a qualitative level, our results reproduce the experimental evolution of the half-lives, i.e., for the $N = 50$ isotones we describe the sharp reduc-

tion of half-lives with decreasing proton number and at the same time, for the Ni isotopes, the gradual reduction of half-lives with increasing neutron number. We give predictions for open-shell nuclei ^{76}Fe and ^{80}Ni near ^{78}Ni that are important for stellar nucleosynthesis. Using the strong tensor correlations [37] our estimation is rather the bottom limit of these half-lives. Also, our calculations show that the influence of the phonon coupling is small on the half-lives of ^{76}Fe and ^{80}Ni .

More information on the β -strength distributions can be derived from simultaneous analysis of the half-lives and the P_n values [45, 46]. Such a program of detailed calculations is underway, the results will be reported in connection to the RIKEN experiments on ^{78}Ni [47].

Acknowledgments

A.P.S., V.V.V., I.N.B and N.N.A thank the hospitality of IPN-Orsay where the part of this work was done. This work is partly supported by the IN2P3-RFBR agreement No. 110291054 and the IN2P3-JINR agreement.

-
- [1] I.N. Borzov, S.A. Fayans, E. Kromer, and D.Zawischa, *Z. Phys.* **A 355**, 117 (1996).
 - [2] J. Engel, M. Bender, J. Dobaczewski, W. Nazarewicz, and R. Surman, *Phys. Rev. C* **60**, 014302 (1999).
 - [3] I.N. Borzov, S. Goriely, *Phys. Rev. C* **62**, 035501 (2000).
 - [4] M. Bender, J. Dobaczewski, J. Engel, and W. Nazarewicz, *Phys. Rev. C* **65**, 054322 (2002).
 - [5] S. Fracasso and G. Colò, *Phys. Rev.* **C76**, 044307 (2007).
 - [6] C. L. Bai, H. Sagawa, H. Q. Zhang, X. Z. Zhang, G. Colò, and F. R. Xu, *Phys. Lett.* **B675**, 28 (2009).
 - [7] C.L. Bai, H.Q. Zhang, H. Sagawa, X.Z. Zhang, G. Colò and F.R. Xu, *Phys. Rev.* **C83**, 054316 (2011).
 - [8] F. Minato and C. L. Bai, *Phys. Rev. Lett.* **110**, 122501 (2013).
 - [9] T. Wakasa, H. Sakai, H. Okamura, H. Otsu, S. Fujita, S. Ishida, N. Sakamoto, T. Uesaka, Y. Satou, M. B. Greenfield, and K. Hatanaka, *Phys. Rev. C* **55**, 2909 (1997).
 - [10] M. Ichimura, H. Sakai, and T. Wakasa, *Prog. Part. Nucl. Phys.* **56**, 446 (2006).
 - [11] G. F. Bertsch and I. Hamamoto, *Phys. Rev. C* **26**, 1323 (1982).
 - [12] V. A. Kuzmin and V. G. Soloviev, *J. Phys.* **G10**, 1507 (1984).
 - [13] S. Drozd, F. Osterfeld, J. Speth, and J. Wambach, *Phys. Lett.* **B189**, 271 (1987).
 - [14] G. Coló, Nguyen Van Giai, P. F. Bortignon, and R. A. Broglia, *Phys. Rev. C* **50**, 1496 (1994).
 - [15] G. Coló, H. Sagawa, Nguyen Van Giai, P. F. Bortignon, and T. Suzuki, *Phys. Rev. C* **57**, 3049 (1998).
 - [16] Y. F. Niu, G. Colò, M. Brenna, P. F. Bortignon, and J. Meng, *Phys. Rev. C* **85**, 034314 (2012).
 - [17] Nguyen Van Giai, Ch. Stoyanov, and V. V. Voronov, *Phys. Rev. C* **57**, 1204 (1998).
 - [18] A. P. Severyukhin, Ch. Stoyanov, V. V. Voronov, and Nguyen Van Giai, *Phys. Rev. C* **66**, 034304 (2002).
 - [19] A. P. Severyukhin, V. V. Voronov, and Nguyen Van Giai, *Phys. Rev. C* **77**, 024322 (2008).
 - [20] V. G. Soloviev, *Theory of Atomic Nuclei: Quasiparticles and Phonons* (Institute of Physics, Bristol and Philadelphia, 1992).
 - [21] A. P. Severyukhin, V. V. Voronov, and Nguyen Van Giai, *Eur. Phys. J.* **A22**, 397 (2004).
 - [22] A. P. Severyukhin, N. N. Arsenyev, and N. Pietralla, *Phys. Rev. C* **86**, 024311 (2012).
 - [23] A. P. Severyukhin, V. V. Voronov, and Nguyen Van Giai, *Prog. Theor. Phys.* **128**, 489 (2012).
 - [24] A. P. Severyukhin and H. Sagawa, *Prog. Theor. Exp. Phys.* **2013**, 103D03 (2013).
 - [25] P. T. Hosmer, H. Schatz, A. Aprahamian, O. Arndt, R. R. C. Clement, A. Estrade, K.-L. Kratz, S. N. Liddick, P. F. Mantica, W. F. Mueller, F. Montes, A. C. Morton, M. Ouellette, E. Pellegrini, B. Pfeiffer, P. Reeder, P. Santi, M. Steiner, A. Stolz, B. E. Tomlin, W. B. Walters, and A. Wöhr, *Phys. Rev. Lett.* **94**, 112501 (2005).
 - [26] A. P. Severyukhin, V. V. Voronov, I. N. Borzov and Nguyen Van Giai, *Rom. Journ. Phys.* **58**, 1048 (2013).
 - [27] P. Ring and P. Schuck, *The Nuclear Many Body Problem* (Springer, Berlin, 1980).
 - [28] T. H. R. Skyrme, *Nucl. Phys.* **9**, 615 (1959).
 - [29] F. Stancu, D. M. Brink, and H. Flocard, *Phys. Lett.* **B68**, 108 (1977).
 - [30] G. Colò, H. Sagawa, S. Fracasso, and P.F. Bortignon, *Phys. Lett.* **B646**, 227 (2007); *Phys. Lett.* **B668**, 457(E) (2008).
 - [31] T. Lesinski, M. Bender, K. Bennaceur, T. Duguet, and J.Meyer, *Phys. Rev. C* **76**, 014312 (2007).

- [32] J. Terasaki, J. Engel, M. Bender, J. Dobaczewski, W. Nazarewicz, and M. Stoitsov, Phys. Rev. C **71**, 034310 (2005).
- [33] G. E. Brown and M. Bolsterli, Phys. Rev. Lett. **3**, 472 (1959).
- [34] P. Sarriguren, E. Moya de Guerra, and A. Escuderos, Nucl. Phys. **A658**, 13 (1999).
- [35] V. O. Nesterenko, J. Kvasil, and P.-G. Reinhard, Phys. Rev. C **66**, 044307 (2002).
- [36] Nguyen Van Giai and H. Sagawa, Phys. Lett. **B106**, 379 (1981).
- [37] C. L. Bai, H. Q. Zhang, X. Z. Zhang, F. R. Xu, H. Sagawa, and G. Colò, Phys. Rev. C **79**, 041301(R) (2009).
- [38] J. Suhonen, *From Nucleons to Nucleus* (Springer-Verlag, Berlin, 2007).
- [39] S. J. Krieger, P. Bonche, H. Flocard, P. Quentin, and M. S. Weiss, Nucl. Phys. **A517**, 275 (1990).
- [40] T. Nikšić, T. Marketin, D. Vretenar, N. Paar, and P. Ring, Phys. Rev. C **71**, 014308 (2005).
- [41] B. Pritychenko, M. Birch, B. Singh, M. Horoi, arXiv:1312.5975v1.
- [42] S. Franchoo, M. Huyse, K. Kruglov, Y. Kudryavtsev, W. F. Mueller, R. Raabe, I. Reusen, P. Van Duppen, J. Van Roosbroeck, L. Vermeeren, A. Wöhr, K. L. Kratz, B. Pfeiffer, and W. B. Walters, Phys. Rev. Lett. **81**, 3100 (1998).
- [43] National Nuclear Data Center, <http://www.nndc.bnl.gov>.
- [44] Z. Y. Xu, S. Nishimura, G. Lorusso, F. Browne, P. Doornenbal, G. Gey, H.-S. Jung, Z. Li, M. Niikura, P.-A. Söderström, T. Sumikama, J. Taprogge, Zs. Vajta, H. Watanabe, J. Wu, A. Yagi, K. Yoshinaga, H. Baba, S. Franchoo, T. Isobe, P. R. John, I. Kojouharov, S. Kubono, N. Kurz, I. Matea, K. Matsui, D. Mengoni, P. Morfouace, D. R. Napoli, F. Naqvi, H. Nishibata, A. Odahara, E. Şahin, H. Sakurai, H. Schaffner, I. G. Stefan, D. Suzuki, R. Taniuchi, and V. Werner, Phys. Rev. Lett. **113**, 032505 (2014).
- [45] I.N. Borzov, Phys. Rev. C **71**, 065801 (2005).
- [46] K. Miernik, K. P. Rykaczewski, C. J. Gross, R. Grzywacz, M. Madurga, D. Miller, J. C. Batchelder, I. N. Borzov, N. T. Brewer, C. Jost, A. Korgul, C. Mazzocchi, A. J. Mendez, Y. Liu, S.V. Paulauskas, D.W. Stracener, J. A. Winger, M. Wolińska-Cichocka, and E. F. Zganjar, Phys. Rev. Lett. **111**, 132502 (2013).
- [47] S. Nishimura, Prog. Theor. Exp. Phys. **2012**, 03C006 (2012).